Evaluation of Reinforced Concrete Bridge Columns Repaired with Fiber Reinforced Polymer Laminates Using Shaking Table Experiments

K.M. Mosalam, P. Kumar, H. Lee, M.S. Günay
University of California, Berkeley

S. Abbasi
CEO, Linford LLC, Covina, CA

SUMMARY
This paper presents an experimental study carried out to evaluate the confinement effectiveness and shear strength and ductility enhancements of Reinforced Concrete (RC) circular bridge columns repaired with Fiber Reinforced Polymer (FRP) laminates as continuous confining media. Two RC columns tested in as-built configurations were ¼-scale models of a prototype bridge column in California. One column had closely spaced hoops satisfying code requirements and the other had widely spaced hoops representing a shear-critical column. The columns were subjected to a series of shaking table tests under the combined effect of horizontal and vertical excitations. Subsequently, the columns were repaired with FRP composite laminates (one with Glass FRP and the other with Carbon FRP) after experiencing moderate flexural damage and moderate to high shear damage. The repaired columns were then subjected to the same set of earthquake excitations. Experimental data showed that the repaired columns achieved higher strength and ductility compared to as-built columns.

Keywords: Bidirectional motion, Bridge columns, FRP repair, reinforced concrete, shaking table.

1. INTRODUCTION

Earthquakes have affected human society in both psychological and physical terms due to their unpredictability. Lack of proper and reliable tools to predict location, time and magnitude of earthquakes contribute to their unpredictable nature. Thus, it is important to develop a scientific understanding of the effects of earthquakes on structures and take precautions against these effects. A number of scientists and engineers have studied both seismological and engineering aspects of earthquakes. From the engineering studies, various pre- and post-earthquake measures have been developed, considering safety, economy and their real world applicability. Pre-earthquake measures stress upon development and application of techniques for safe and reliable seismic design of structures. In most of the cases, post-earthquake measure suggests two main options: demolition of damaged structure or their repair.

Demolition of structures can become important in two main situations:
(a) The site is rendered unsafe for future use because of seismic activity in that specific region.
(b) The structure underwent severe and widespread damage and constructing a new structure is beneficial from both economical and safety point of view.

Due to recent advancements in structural and earthquake engineering, most of the new structures are designed to avoid collapse by concentrating damage in sacrificial regions, e.g. plastic hinges. Such structures can be repaired after an earthquake, without demolition, in practical and effective ways. Following are few main advantages of repairing a structure after earthquake over their demolition:
(1) More economical even when structural members experienced nonlinear deformations;
(2) Less time is needed for repairing damaged regions and curing process is more efficient; and
(3) Research activities showed higher stiffness, ductility, and strength of repaired systems.

Two pre-damaged Reinforced Concrete (RC) circular bridge columns were chosen for this research. Both test specimens were identical except for the volumetric transverse reinforcement ratio due to

different spacing of hoop reinforcement in the two specimens. The two test specimens were retrofitted using Glass and Carbon Fiber Reinforced Polymer (GFRP and CFRP) jackets. The repaired specimens were tested on a shaking table. The goals of this experimental study were:

(1) To investigate response of repaired RC circular bridge columns subjected to series of horizontal and vertical ground motions; and
(2) To compare the response of repaired and as-built specimens.

2. AS-BUILT AND REPAIRED TEST SPECIMENS

A previous research was conducted to investigate the effect of vertical ground motions on shear demand and capacity of two as-built ¼-scale RC circular bridge column specimens (Lee 2011). Both test specimens had identical geometry and reinforcement details except their volumetric transverse reinforcement ratios. Test specimen SP1 had closely spaced transverse reinforcement than test specimen SP2. Axial load ratio was 6.8% of the nominal axial load capacity for both test specimens considering a nominal compressive concrete strength, $f'_c = 3.9$ ksi. As-built test specimens were subjected to a series of horizontal and vertical ground motions on a shaking table.

The Plumas Arboga overhead was chosen as the prototype for the two as-built test specimens. Fig. 2.1 shows the elevation and section views of the prototype column, showing the geometrical and reinforcement details. The bridge is a three-span bridge with single column bents having interior span of 190 ft and exterior span of 133 ft. Test specimens were scaled down by approximately ¼-scale keeping the aspect ratio, i.e. height to diameter ratio, of 3.5.

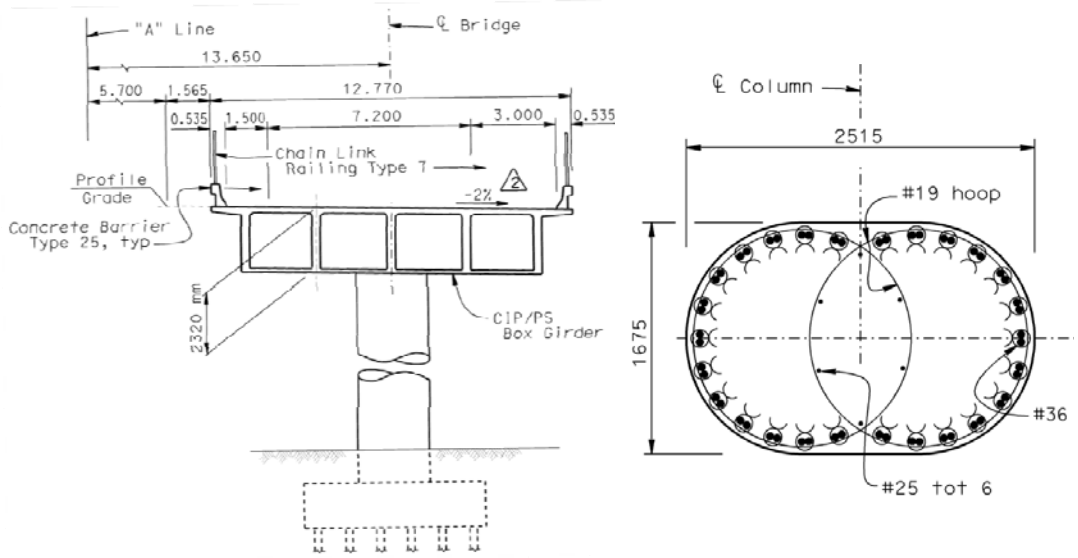

a) Elevation (Dim. in m, unless noted otherwise) b) Cross-section (Dim. in mm)

Figure 2.1 Plumas Arboga overhead prototype bridge column (Plumas 2010).

Fig. 2.2 shows both the section and elevation views of the specimens SP1 and SP2. Test specimen SP1 had a diameter of 20 in. and height of 70 in. The longitudinal reinforcement consisted of 16 #5, A706, bars distributed uniformly around the perimeter, resulting in a longitudinal steel ratio of ρ_l = 1.56%. #2 deformed steel reinforcement hoops were used at 2 in. center-to-center spacing, leading to a volumetric transverse reinforcement ratio of ρ_v = 0.55%. The clear cover thickness of concrete was 1.0 in. Test specimen SP2 had the same geometrical and reinforcement details except for the spacing of #2 hoops was increased to 3 in. center-to-center, with corresponding volumetric transverse reinforcement ratio of ρ_v = 0.36%. Nominal shear strength values (ACI 2008; Caltrans 2004) of SP1 and SP2 were 79.41 and 50.51 kips, respectively. These values were computed using a displacement ductility demand, μ_d = 4.0, following procedures outlined in (Caltrans 2006). Both SP1 and SP2 had their

transverse hoop reinforcement extended into the foundation and the top blocks, as shown in Fig. 2.2. The center-to-center spacing in these regions was kept equal to the spacing in the column region. The ratios of the transverse reinforcement spacing to the longitudinal bar diameter were 3.2 and 4.8 for SP1 and SP2, respectively, in order to avoid buckling of longitudinal reinforcement.

The footing was designed to avoid any shear or punching failures during testing (Lee 2011). The footing size was 60 in. × 60 in. × 18 in. where the depth of footing was more than the development length of the longitudinal reinforcing bars that were extended into it to avoid any bar slip. The footing was firmly connected to the shaking table using post-tensioning rods to avoid any decompression under maximum expected overturning moment and to prevent sliding at maximum shear transfer relative to the shaking table. The top mass block was designed and detailed to remain undamaged during the shaking table testing (Lee 2011). Eight PVC pipe holes running in each of the two perpendicular directions were prepared during the construction and steel tubular beams (used to attach lead blocks for additional mass for scale-compensation) were post-tensioned to the top block using threaded rods (Lee 2011).

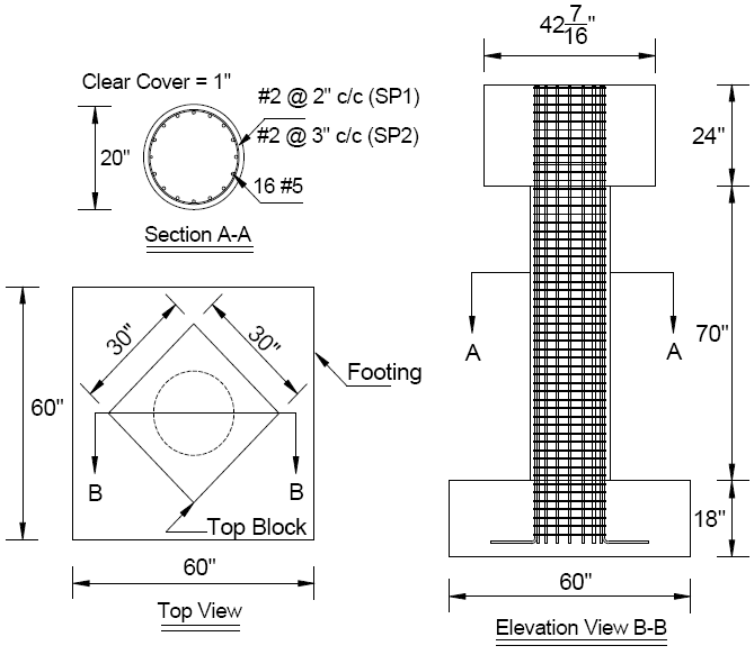

Figure 2.2 Section, elevation and top view of the test specimens.

Fig. 2.3 shows both the top and elevation views of the test specimens. Total weight on the top of the specimens was 85.6 kips which gave the required axial load ratio of 6.8%. Four Hollow Steel Section (HSS) beams were attached on the four sides of the top block where each beam was loaded with 4, 6, or 8 stacks lead blocks, Fig. 2.3b. On top of this lead mass configuration, two concrete slabs were attached. The top slabs were firmly connected to the HSS beams using post-tensioning steel rods. In addition, the lead block masses and steel beams were connected in a similar manner. These post-tensioning rods were subjected to pre-stressing force high enough to avoid slippage between the connected elements. The center of gravity of the superstructure mass was located at 4.45 in. above the circular column and top block intersection. The mass moment of inertia of the test specimens was 45 kips.ft.s^2. The superstructure mass configuration was chosen to match the ¼-scale values of the same parameters for the prototype bridge column. Pre-analysis of the test specimens showed that their lateral vibration period was comparable to that of the scaled version of the prototype bridge column.

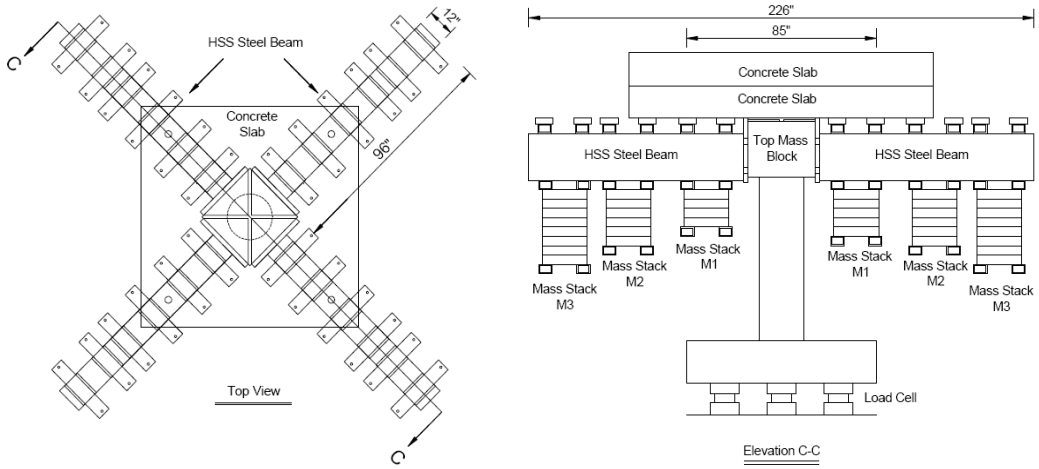

a) Top plan view b) Elevation view

Figure 2.3 Superstructure Mass Configurations.

Both as-built test specimens were subjected to the same set of horizontal and vertical ground motions and they developed shear and flexure cracks, with more damage in as-built specimen SP2 compared to SP1, Fig. 2.4(a) and (b). Both damaged columns were repaired by the same standard procedure.

(a) Damage state of as-built specimen SP1

(b) Damage state of as-built specimen SP2

(c) Hammer test to remove lose material

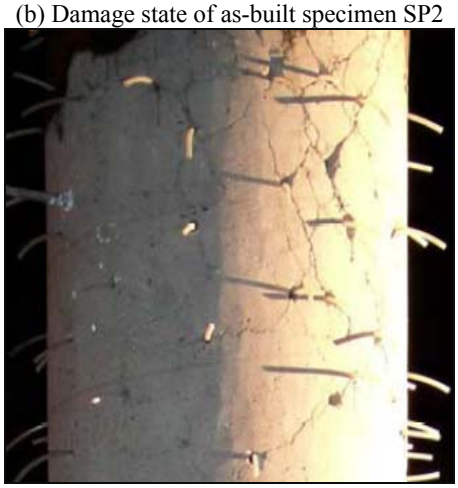

(d) Injection ports in damaged regions

Figure 2.4 Repair of test specimens (preparation stage).

Using the sounding hammer test, lose and unsound concrete was mechanically removed from the columns surface, Fig. 2.4(c). Using wire brushes the exposed parts of the reinforcing bars were cleaned of any rust. Injection ports were installed in all cracks at adequate spacing. Bonding and protection system were applied on cleaned concrete and reinforcement surfaces, Fig. 2.4(d). Voids wider than ¾ in. were patched using structural mortar and those smaller than ¾ in. were cap sealed using gel/paste epoxy system, Fig. 2.5(a). After the cap seal and patch material were cured, structural epoxy system was injected in all cracks. Multi-port injection system was used with relatively low pressure to prevent expansion and further damage to cracked concrete, Fig. 2.5(b). When injection resin was cured, specimen surfaces were grinded to remove cap seal material and injection ports. Surface was then cleaned of any dust debris and one coat of prime was applied. Four layers of unidirectional GFRP composite system impregnated with structural epoxy system were installed on damaged specimen SP1, Fig. 2.5(c). On the other hand, two layers of unidirectional CFRP composite system impregnated with structural epoxy system were installed on damaged specimen SP2, Fig. 2.5(d). Temporary polyvinyl compression/curing tapes were wrapped on the installed FRP.

Among the various possible ways of retrofitting with jackets, simple technique of wrapping was chosen. The repair was oriented towards ductility improvement. After testing of the as-built columns, both columns experienced moderate to severe damage. The shear-critical column SP2 had more damage than SP1. Therefore, CFRP with higher tensile strength than GFRP was used for SP2 and GFRP was used for SP1.

(a) Cap sealing and surface repair

(b) Multiport injection system

(c)) GFRP repaired SP1

(d) CFRP repaired SP2

Figure 2.5 Repair of test specimens (FRP application).

The number of layers of each jacket was determined based on section analyses. The final stiffness from global force-deformation relationships of the as-built specimens (Lee 2011) were as follows:

- 57.0 kips/in (positive side), 105.4 kips/in (negative side) and 81.2 kips/in (average) for SP1; and

- 55.0 kips/in (positive side), 88.2 kips/in (negative side) and 71.6 kips/in (average) for SP2.

To achieve a target drift ratio of at least that of the as-built specimens, i.e. 2% for SP1 and SP2, section design was carried out, requiring jacket thickness for SP1 and SP2 of 0.140″ and 0.065″, respectively. Since the thickness of each layer of the CFRP and GFRP was 0.04″, four layers of GFRP were used for SP1 and two layers of CFRP were used for SP2.

The average compressive strength of concrete on the day of testing of the as-built specimens was 3.88 ksi. The maximum size of the coarse aggregates was ¾ in. and the average density of concrete mix was 150.3 pcf. Longitudinal reinforcement bars made of 16#5, confirming to ASTM A706, were used in both test specimens SP1 and SP2. The yield strength of the reinforcement was 68 ksi and the ultimate stress at bar fracture was 96 ksi. The #2 deformed bars hoops were used for confinement. The hoops were lap welded at ends. The yield strength of the #2 deformed bars was 63 ksi. Reinforcement used for the footing and top mass block was Grade 60 steel conforming to ASTM A615.

GFRP composite system, consisting of unidirectional structural glass fabric and fiber impregnation resin, was installed on damaged as-built test specimen SP1. Average laminate tensile strength was 90.76 ksi with rupture strain of 2.3%. CFRP composite system, consisting of unidirectional structural carbon fabric and fiber impregnation resin, was installed on damaged as-built test specimen SP2. Average laminate tensile strength was 143.95 ksi with an average tensile modulus of 9000 ksi. Thickness plies for both GFRP and CFRP was 0.04 in.

3. EXPERIMENTAL SETUP AND TEST PROGRAM

The testing of both repaired specimens was carried out using the PEER shaking table, Fig. 3.1. A stiff steel plate of dimensions 8 ft × 8 ft × 3.35 in. was attached to the shaking table to be able to center the test specimen on the shaking table. The test specimen was attached to the steel plate with four load cells placed between the bottom of the specimen footing and the top of the steel plate. The load cells were placed near the four corners of the footing of test specimen to measure the reaction components between the table and the column. The test specimens were instrumented both internally and externally using strain gauges, displacement transducers, accelerometers and wire-potentiometers.

Figure 3.1 Setup of test specimen repaired with GFRP composite.

The same set of horizontal and vertical ground motions as that used in testing of as-built specimens was applied to the repaired columns. The ground motion recording, different scales of which constitutes the applied ground motion set, has previously been determined from the fidelity tests conducted on the shaking table using mass blocks which had approximately the same weight and center of gravity location as the test specimens (Lee 2011). Pacoima Dam recording of the 1994 Northridge earthquake which was successfully reproduced during these fidelity tests was chosen amongst four different sets of filtered two-dimensional (2D) ground motions, which were determined based on the analyses of a single column of the previously mentioned prototype bridge. Table 3.1 lists the details of the loading protocol where a series of horizontal only, and horizontal and vertical motions were applied using scaling of the originally recorded ground motions. It is noted that the as-built test specimen SP1 was not tested for EQ4 and EQ6, identified in Table 3.1.

Table 3.1 Ground motion selection for shaking table testing (PEER 2007).

Test	Earthquake	Station	Scale Factor	Components
EQ1	Northridge	Pacoima Dam	0.050	Horizontal and vertical
EQ2	Northridge	Pacoima Dam	0.125	Horizontal and vertical
EQ3	Northridge	Pacoima Dam	0.250	Horizontal and vertical
EQ4	Northridge	Pacoima Dam	0.250	Horizontal only
EQ5	Northridge	Pacoima Dam	0.500	Horizontal and vertical
EQ6	Northridge	Pacoima Dam	0.500	Horizontal only
EQ7	Northridge	Pacoima Dam	0.700	Horizontal and vertical
EQ8	Northridge	Pacoima Dam	0.950	Horizontal and vertical
EQ9	Northridge	Pacoima Dam	1.250	Horizontal and vertical
EQ10	Northridge	Pacoima Dam	1.250	Horizontal only
EQ11	Northridge	Pacoima Dam	1.250	Horizontal and vertical

4. EXPERIMENTAL RESULTS

Both repaired specimens showed improved stiffness and ductility compared to the as-built specimens. Calculations of shear force are performed from the data obtained using the load cells below the footings. Relative displacements were calculated from the wire-potentiometers data, after verification. Drift ratio was calculated as the ratio of measured displacement to the height of the test specimen. The FRP repair jacket of both test specimens was intact during the entire testing runs. The comparison of the force-deformation plots of the repaired and as-built specimens is presented in Fig. 4.1, where it is observed that the repaired test specimens resisted shear force greater than or equal to that resisted by the as-built test specimens. Plots of strain profiles measured from strain gauge data and vertical displacement transducers are also presented. It was observed that the FRP jackets remained intact in both of the repaired specimens with minor damage and negligible residual displacements.

4.1 Test Specimen SP1

The effectiveness of confinement was more obvious for the ground motions with higher scale factors. Figures 4.1(a) and (c) show the force-deformation response of the repaired SP1 subjected to EQ9 and EQ10 (Table 3.1). Figures 4.2(b) and (d) show the comparisons with the as-built SP1. Under both of these high ground motions, the repaired SP1 was stiffer than that of the as-built SP1 and was able to resist slightly higher shear forces. In general, the repaired column resisted comparatively more shear force and also had higher stiffness as compared to the as-built case under all levels of ground motion.

Based on the strain measurements of the longitudinal reinforcement, the first yielding of the reinforcing bars occurred during ground motion EQ5 (Table 3.1) near the top of the column. For all ground motions afterwards, strain values were higher and yielding spread along the column height. In the last ground motion (EQ11 of Table 3.1), all the strain gauges above the mid-height of the column measured strains greater than the yield strain of the steel reinforcement. For the high intensity ground motions, the curvature diagram, derived from the displacement measurements at the opposite sides of various cross-sections along the column height, suggested double curvature behavior, which was also supported by the measurements of the strain gauges readings. Moreover, the longitudinal strains in the

reinforcement were tension above the mid-height of the specimen and they were compression for the portion of reinforcement below the mid-height cross-section.

Fig. 4.2 shows the strain profiles measured using the strain gauges attached on the GFRP jacket around the test specimen circumference. These plots are referred to as "polar strain profile plots." The markers shown on the plots correspond to the time when maximum strain was measured along the column height at any of the strain gauge locations. The origin of the plot represents the center of the column cross-section and the radial grid lines represent the angular locations (in degrees) of the strain gauges measured with respect to the north direction (note that applied horizontal ground motion was north-south). Circles represent the strain value increasing with the increase of the radial direction.

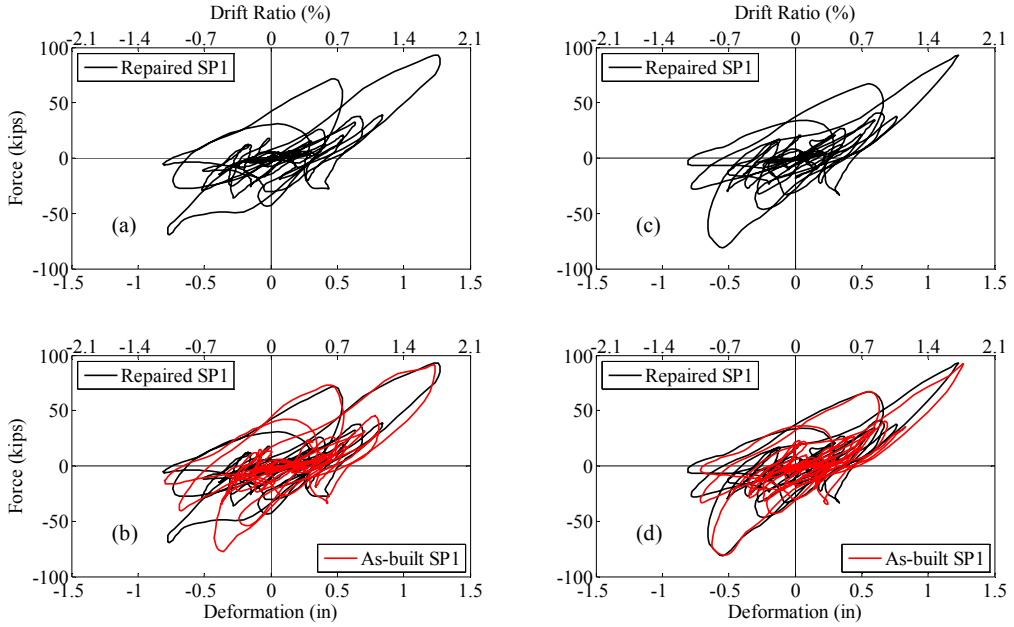

Figure 4.1 Force-deformation responses of SP1: (a) EQ9, (b) EQ9 comparison, (c) EQ10, (d) EQ10 comparison.

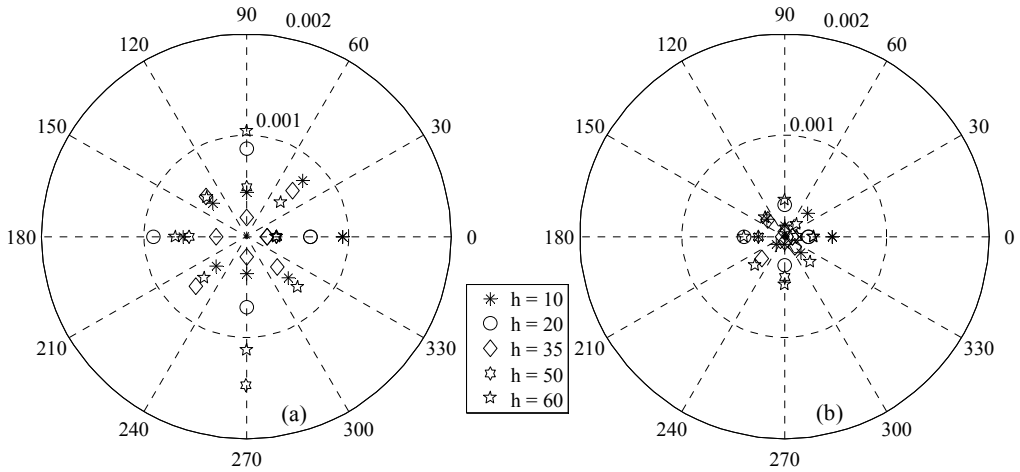

Figure 4.2 Strain profiles of SP1 from jacket strain when max. strain occurs along height: (a) EQ9, (b) EQ10.

4.2 Test Specimen SP2

Fig. 4.3 shows the force-deformation response of repaired and as-built SP2 under EQ9 and EQ10 (Table 3.1). Due to improved confinement configuration provided by the FRP jacket repair, the

repaired SP2 was more ductile, had higher stiffness, and resisted higher base shear compared to the as-built SP2. The effect of the CFRP repair on enhancing the shear capacity of a column with relatively large hoop spacing is clearly observed.

The curvature behavior was similar to that observed for the repaired specimen SP1. One main difference was that the first yield occurred near the top of the column during EQ6 (Table 3.1). The spreading of yield strain along the repaired SP2 height was gradual compared to the repaired SP1. However, both repaired specimens had comparable response for higher intensity earthquakes.

Fig. 4.4 shows the strain profiles measured using the strain gauges attached on the GFRP jacket around the test specimen circumference. The markers shown on the plots correspond to the time when maximum strain was measured along the column height at any of the strain gauge locations.

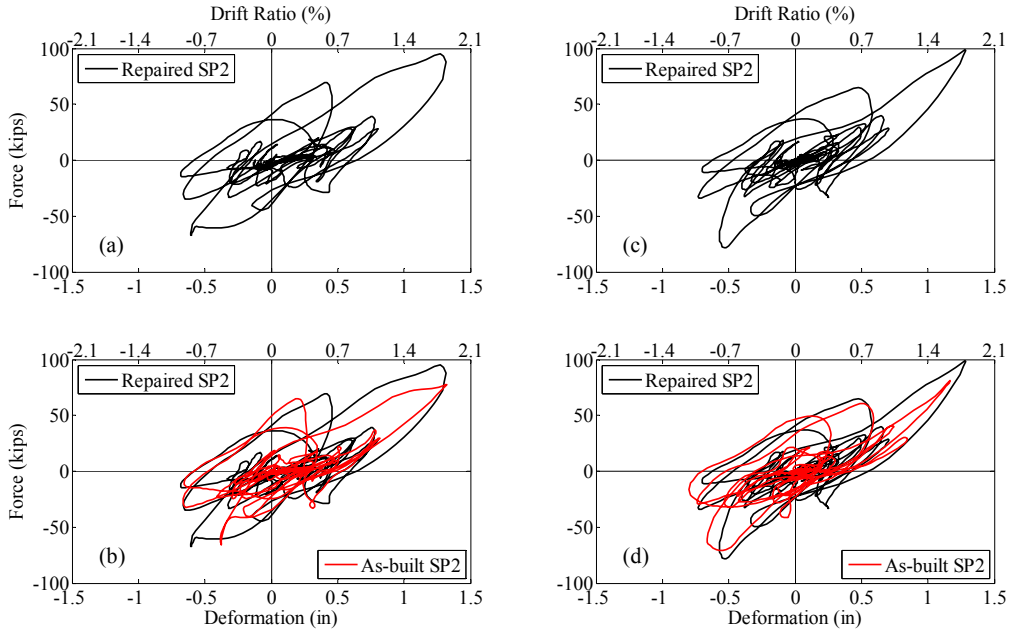

Figure 4.3 Force-deformation responses of SP2: (a) EQ9, (b) EQ9 comparison, (c) EQ10, (d) EQ10 comparison.

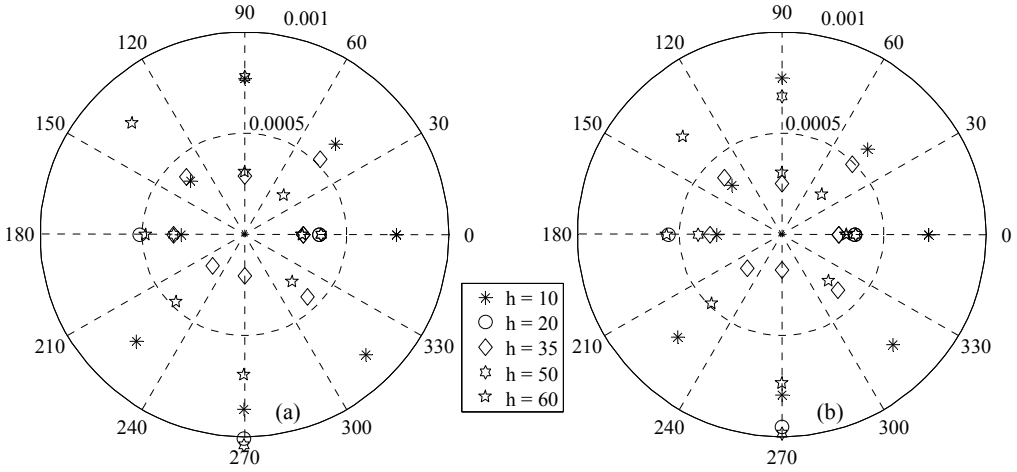

Figure 4.4 Strain profiles of SP2 from jacket strain when max. strain occurs along height: (a) EQ9, (b) EQ10.

5. CONCLUSIONS

Based on the experimental investigations of the seismic response of two FRP repaired columns in comparison with their as-built column counterparts, under the effect of both horizontal and "horizontal and vertical " ground motions, following conclusion can be deducted:

1. Force-deformation response of GFRP repaired specimen was very similar to its as-built counterpart. Considering that the as-built specimen was code compliant in terms of transverse reinforcement and accordingly did not experience severe damage during testing, the improvement provided by GFRP repair by upgrading the response of the damaged as-built specimen to its original undamaged response state is beneficial.
2. The CFRP repaired specimen showed an improved force-deformation response compared to its as-built counterpart, especially in terms of strength. The effect of the CFRP repair on enhancing the shear capacity of a column with relatively large hoop spacing was remarkable.
3. Both of the repaired test specimens were successful in providing the required passive confinement after the damage. Under the test ground motions no shear failure of retrofit jackets was observed, which is also justified by the strain measurements on the jackets.
4. For both of the repaired specimens, residual displacement was quite small and FRP jacket was intact during the entire testing runs.
5. Complementary to the above conclusions, it can be stated that the FRP repair is a viable repair solution regarding the shear strength of bridge columns under the adverse effects of vertical ground motion excitations. Similarly, bridge columns which are shown to be underperforming by analytical methods or other means can be retrofitted by FRP jackets in order to overcome the shear strength reduction caused by vertical excitations.

ACKNOWLEDGEMENTS

The research was supported by Caltrans under Award Number 07-003895-UCB. PEER Center staff assistance was essential for the experimental study. Linford LLC has made valuable contributions of the FRP repair design and materials. Perse Construction Company has helped with the application of the FRP and repairs.

REFERENCES

ACI Committee (2008). Building Code Requirements for Structural Concrete and Commentary, American Concrete Institute, Farmington Hills, MI.

Caltrans (2004). Bridge Design Specifications, California Department of Transportation, Sacramento, CA.

Caltrans (2006). Seismic Design Criteria, California Department of Transportation, Sacramento, CA.

Lee, H. (2011). Experimental and Analytical Investigation of Reinforced Concrete Columns Subjected to Horizontal and Vertical Ground Motions. *PhD dissertation*, Univ. of California, Berkeley, CA.

PEER (2007). PEER Strong Motion Database: Introduction. http://peer.berkeley.edu/smcat

Plumas Arboga Drawing Sheets (2010). Bridge Inspection Records Information System, Division of Maintenance, California Department of Transportation, Sacramento, CA.